This article has been accepted for publication in a future issue of this journal, but has not been fully edited. Content may change prior to final publication. Citation information: DOI 10.1109/TMAG.2015.2449779, IEEE Transactions on Magnetics

Effect of Mechanical Stress on Excess Loss of Electrical Steel Sheets

Deepak Singh[1], Paavo Rasilo[1], Floran Martin[1], Anouar Belahcen[1], and Antero Arkkio[1]

[1]Department of Electrical Engineering and Automation, Aalto University School of Electrical Engineering, P.O. Box. 13000, FI-100076 Espoo, Finland

Effect of mechanical stress on the magnetic loss of electrical steel sheets is analyzed utilizing the statistical loss theory. The focus of the study is on the variation of the excess loss component with the applied stress and its correlation with the hysteresis loss. The model and its correlation are validated by performing comprehensive measurements at various combination of induction levels, frequencies and stresses. It is found that the excess losses can be modeled with sufficient accuracy by their correlation with the hysteresis losses over a wide range of stresses, frequencies and flux densities.

Index Terms—**Excess loss, hysteresis loss, magnetic materials, single sheet tester, stress.**

I. Introduction

MAGNETIC properties of electrical steels are known to deviate significantly under stress. The characteristic curves and the loss coefficients, that define the properties of the electrical steel, are typically determined by some standardized test process with no external stress [1], [2]. However, in an electrical machine the stress state of these materials is never zero. Shrink-fitting and the magnetic and centrifugal forces exert considerable stress on the iron cores of electrical machines [3]. Various previous studies have reported the deviation in the magnetic characteristics and the power loss densities when the material is under mechanical stress [4]–[6]. The theory of coercive field [7], based on the statistical analysis of the magnetic objects, provides a strong dependency between coercive field and the magnetostrictive strain. From this coercive field and the first magnetization curve, the hysteresis losses can be determined and correlated to the applied stress. Furthermore, in [8] the stress dependency of the parameters representing the intrinsic material properties in the statistical iron loss model [9] has been presented. However the study was based on measurements only at a single frequency.

In this study, measurements from a modified single sheet tester (SST) with a provision of unidirectional stressing, are used to analyze the stress dependency of the above mentioned parameters of the statistical iron loss model. The measurements for this study were carried out at various stresses (both compressive and tensile), magnetic inductions and frequencies. A strong correlation between the hysteresis loss variation with stress and excess loss component was observed. This correlation was further utilized to model the excess power loss over the whole range of data.

II. Methodology

A. Statistical Loss Theory and Loss Segregation

The fundamental premise for the statistical loss theory is the movement of magnetic objects (MOs) which depict a number of magnetic domain walls transitioning in a highly correlated manner [10]. Based on the microscopic and macroscopic levels of magnetization process in these MOs, the applied magnetic field H that induces a uniform induction, is segregated into hysteresis H_{hy}, classical eddy current H_{ed} and excess fields H_{ex}. Similarly, the total power loss P_{tot} is dissociated into components corresponding to these respective fields (*i.e.* P_{hy}, P_{ed} and P_{ex}).

P_{hy} can be obtained by the quasi-static measurement *i.e.* at low frequency f or by extrapolating the energy loss per cycle to zero frequency ($f \to 0$).

$$\frac{P_{\text{hy}}}{f} = W_{\text{hy}} = \lim_{f\to 0} W_{\text{tot}} \tag{1}$$

$$H_{\text{hy}} = \frac{P_{\text{hy}}}{4B_{\text{p}}f}, \tag{2}$$

where W_{hy} and W_{tot} are the hysteresis and total energy loss per cycle, respectively. H_{hy} is the average hysteresis field for a sinusoidal induction and B_{p} is the peak induction [9]. Assuming uniform penetration of magnetic flux, the classical eddy current power loss component P_{ed} can be determined analytically as a function of the peak induction B_{p} and the frequency that includes the material conductivity λ and the thickness d of the lamination [11]:

$$P_{\text{ed}} = \frac{\lambda\pi^2 d^2 B_{\text{p}}^2 f^2}{6}. \tag{3}$$

Finally, the excess power loss (P_{ex}) can be segregated from the measured total loss (P_{tot}) as

$$P_{\text{ex}} = P_{\text{tot}} - P_{\text{hy}} - P_{\text{ed}}. \tag{4}$$

For the sinusoidal induction, the time averaged excess field H_{ex} can be expressed as [9]

$$H_{\text{ex}} = \frac{P_{\text{ex}}}{4B_{\text{p}}f}. \tag{5}$$

B. Excess Loss Models

From the statistical loss theory [10], the time averaged approximation of the number of simultaneously active MOs

Manuscript received March 20, 2015. Corresponding author: D. Singh (email: deepak.singh@aalto.fi).

This article has been accepted for publication in a future issue of this journal, but has not been fully edited. Content may change prior to final publication. Citation information: DOI 10.1109/TMAG.2015.2449779, IEEE Transactions on Magnetics

(*i.e.* n) for the sinusoidal induction in a cross section S of the lamination is given by

$$n = \frac{2\pi^2 \lambda G S B_{\mathrm{p}}^2 f^2}{P_{\mathrm{ex}}}, \tag{6}$$

where $G = 0.1356$ is a model constant [11]. In [9], [10], and [12] a linear correlation between n and H_{ex}, was obtained from measurements for non-oriented electrical sheets and grain oriented sheets with respect to the rolling direction. Thus, the number of simultaneously active MOs can also be expressed as

$$n = n_0 + \frac{H_{\mathrm{ex}}}{V_0}, \tag{7}$$

where n_0 represents the number of active MOs at the quasi-static state, and V_0 is the characteristic field that governs the increase of the active MOs due to the external field. Consequently, P_{ex} is deduced as [11]

$$P_{\mathrm{ex}} = 2B_{\mathrm{p}} f \left(\sqrt{n_0^2 V_0^2 + 2\pi^2 \lambda G S B_{\mathrm{p}} f V_0} - n_0 V_0 \right). \tag{8}$$

Analyzing the intrinsic material parameters n_0 and V_0 fitted to the measured data can reveal various magnetic properties of the material. In [9] n_0 was neglected for the non-oriented steel based on the measured results. The physical interpretation was owed to the fact that in non-oriented steel any memory regarding the MOs orientation in the quasi-static state is quickly destroyed. Following this assumption, (8) for non-oriented steel reduces to

$$P_{\mathrm{ex}} = \sqrt{8\pi^2 \lambda G S V_0}\ B_{\mathrm{p}}^{1.5} f^{1.5}. \tag{9}$$

C. Model Parameters and Stress Dependency

The effect of tensile stress on the model parameters n_0 and V_0 for the grain oriented electrical steel (annealed and plastically deformed), was first reported in [12]. The study concluded that the effect of tensile stress is a stress induced domain refinement as well as a more coherent motion of the domain wall. The parameter V_0 was approximated to be proportional to H_{hy} upon stress application. In [8] a clear correlation (in a wide range of stress) in the trend of the hysteresis loss vs stress and V_0 vs stress was observed. However the analysis was done with the measured data at a single induction level and one frequency only. In our study, we investigate this correlation at various induction levels and frequencies, and obtain a comprehensive stress dependent iron loss model for the non-oriented material under consideration.

For the analysis, the stress dependency and a linear relation between the parameter V_0 and H_{hy} are introduced in the model. Two variants of the stress dependent excess loss model, namely *Model 1* and *Model 2*, are derived from equations (8) and (9) respectively. In *Model 1*

$$P_{\mathrm{ex}}(B_{\mathrm{p}}, f, \sigma) = 2B_{\mathrm{p}} f \left(\sqrt{\left(n_0(\sigma) V_0\right)^2 + 2\pi^2 \lambda G S B_{\mathrm{p}} f V_0} - n_0(\sigma) V_0 \right) \tag{10}$$

$$V_0(B_{\mathrm{p}}, \sigma) = \frac{1}{k_1} H_{\mathrm{hy}}(B_{\mathrm{p}}, \sigma) = \frac{W_{\mathrm{hy}}(B_{\mathrm{p}}, \sigma)}{4 k_1 B_{\mathrm{p}}}, \tag{11}$$

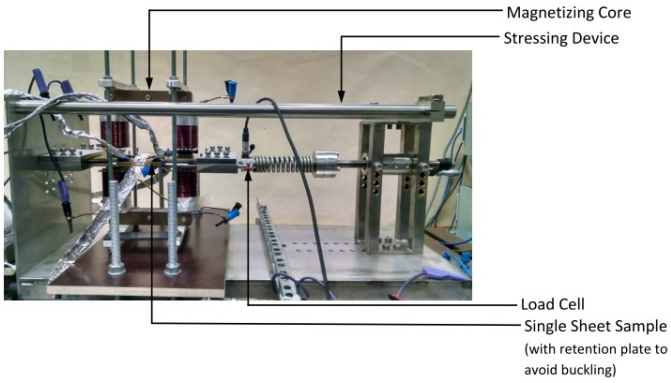

Fig. 1. Measurement setup for unidirectional magnetization and co-linear stress

σ is the applied external stress and k_1 is a proportionality constant which is fixed to a single value for the whole range of measurement combinations. The stress dependent parameter $n_0(\sigma)$ is identified separately for each stress value. On the other hand in *Model 2*

$$P_{\mathrm{ex}}(B_{\mathrm{p}}, f, \sigma) = \sqrt{8\pi^2 \lambda G S V_0}\ B_{\mathrm{p}}^{1.5} f^{1.5} \tag{12}$$

$$V_0(B_{\mathrm{p}}, \sigma) = \frac{1}{k_2} H_{\mathrm{hy}}(B_{\mathrm{p}}, \sigma) = \frac{W_{\mathrm{hy}}(B_{\mathrm{p}}, \sigma)}{4 k_2 B_{\mathrm{p}}}, \tag{13}$$

only the proportionality constant k_2 is fixed to a single value for the whole range. However, it is important to mention that the constants k_1 in *Model 1* and k_2 in *Model 2* might have different values.

III. Measurement Setup

Fig. 1 shows the magnetization core and the SST sample along with the custom-built stressing device having a range and resolution of ± 1250 N and 1 N, respectively. A programmable power source and a data acquisition system (DAQ) with analog output were used in conjunction with a PC to control the magnitude and waveform of the supply voltage so as to produce a sinusoidal induction in the SST sample. The feedback control of the supply voltage was programmed using MATLAB/DAQ toolbox. In addition to that, a high speed DAQ system and low-noise/high-gain signal amplifiers were used to retrieve the measured signals for the field strength and the flux density. Tunneling magneto-resistance (TMR) sensors arranged in a 2×2 grid were used to measure the surface magnetic field strength, and a coil wound around the sample was used to measure the magnetic flux density.

IV. Results

The measured single sheet sample was cut along the rolling direction of M400-50A grade fully processed non-oriented electrical steel sheet. The measurements were done for the stress range of -40 MPa (compressive) to 100 MPa (tensile) and the frequency range of 0.2 Hz to 100 Hz. In order to negate the skin effect, the maximum supply frequency was limited to 100 Hz.

This article has been accepted for publication in a future issue of this journal, but has not been fully edited. Content may change prior to final publication. Citation information: DOI 10.1109/TMAG.2015.2449779, IEEE Transactions on Magnetics

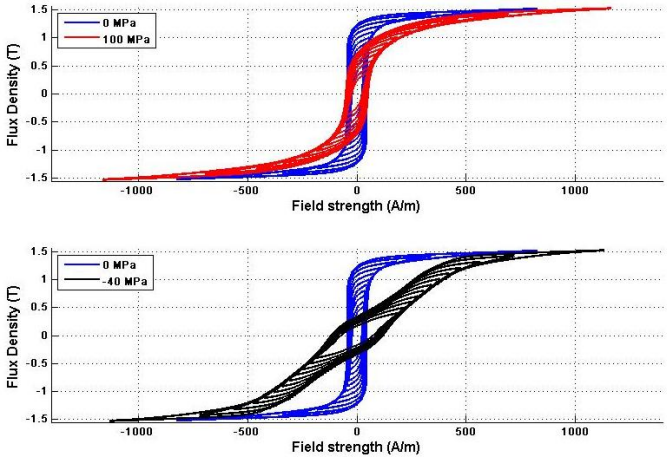

Fig. 2. Deformation in BH-loops due to stress (at $f = 20$ Hz)

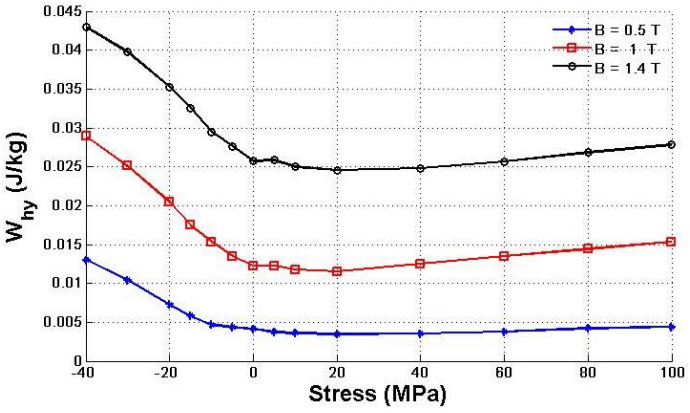

Fig. 3. Variation of measured W_{hy} with respect to stress

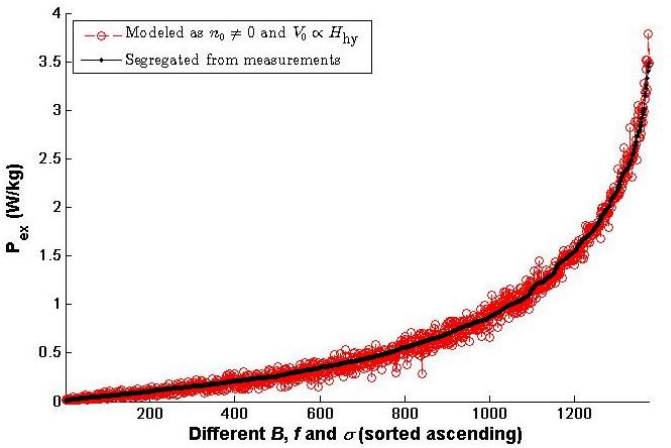

Fig. 4. Excess loss measured and modeled using *Model 1*

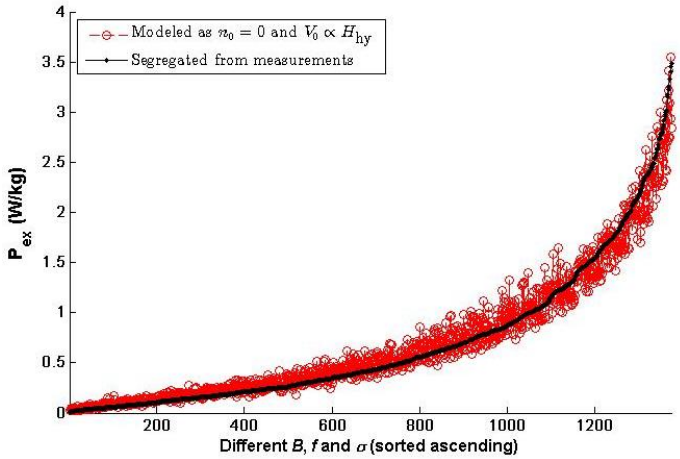

Fig. 5. Excess loss measured and modeled using *Model 2*

A. Loss Measurements and Segregation

Significant deformation in the BH-loops were observed when the steel sheet sample was stressed. Fig. 2 shows an example of the deformation of the BH-loops with respect to the zero stress condition at various induction levels ($B_{\text{p}} = 0.4 - 1.5$ T). The total power loss for each measurement combination was calculated from the measured signals of the field strength H_{mes} and the flux density B_{mes} as

$$P_{\text{tot}} = f \int_0^{\frac{1}{f}} H_{\text{mes}} \frac{\mathrm{d}B_{\text{mes}}}{\mathrm{d}t}\, \mathrm{d}t. \tag{14}$$

Since the uniformity of the flux penetration in the measured sheet sample was ensured by limiting the maximum frequency (*i.e.* eliminating the skin effect), the classical eddy current loss was estimated using the analytical expression (3). Furthermore, assuming $P_{\text{tot}} \approx P_{\text{hy}}$ at very low frequencies (*i.e.* $f = 0.2$ Hz and 0.5 Hz), the energy loss per cycle W_{hy} and the hysteresis power loss P_{hy} for various induction levels were determined from the measurements. Fig. 3 shows the variation of measured W_{hy} with respect to the applied external stress at different induction levels.

B. Excess Loss Models Fitting

Following the determination of P_{hy} and P_{ed}, the excess loss P_{ex} was segregated using (4). The segregated P_{ex} from the measurements were then fitted against the excess loss models *Model 1* and *Model 2*. As explained earlier, the fitting was done assuming the parameter $V_0 \propto H_{\text{hy}}$. Fig. 4 and 5 show the excess power loss segregated from the measurements and the modeled results using *Model 1* and *Model 2*, respectively. The data points are at various measurement combinations of the induction levels, frequencies and stresses, arranged in ascending order of the excess power loss segregated from the measurements. The best fit of the modeled and segregated excess loss was obtained at the proportionality constant values of $k_1 = 10$ and $k_2 = 16.28$. Fig. 6 shows the variation of the parameter n_0 obtained from *Model 1* fitting (which represents the number of active MOs at quasi-static state) with the applied stress.

V. Discussion

A. Loss Segregation

One of the important issues with the validation of models was the accurate segregation of the excess loss. The

This article has been accepted for publication in a future issue of this journal, but has not been fully edited. Content may change prior to final publication. Citation information: DOI 10.1109/TMAG.2015.2449779, IEEE Transactions on Magnetics

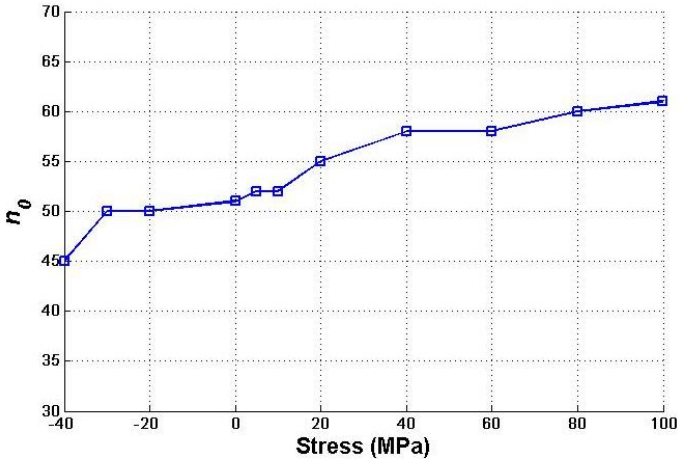

Fig. 6. Stress dependency of parameter n_0 in *Model 1*

hysteresis energy loss W_{hy} and consequently P_{hy} estimation (or extrapolation) from higher frequency measurement ($f = 2$ Hz or 5 Hz) resulted in very erroneous segregation of the excess power loss P_{ex}. The measurements at very low frequencies (*i.e.* $f = 0.2$ Hz and 0.5 Hz) were specifically done to overcome this issue.

B. Models Fitting

As analyzed in section III-C of [12] and the results of [8], the observation $V_0 \propto H_{\text{hy}}$ was found to be valid for the whole range of the measurement combinations in both *Model 1* and *Model 2*. Contrary to the conclusion of [12], a drastic change in the parameter n_0 when under tensile stress was not observed (Fig. 6). This observation of drastic jump in the parameter n_0 under tensile stress [12] was made for a grain oriented steel. Nevertheless, from Fig. 6 a clear trend in the variation of n_0 with the stress can be observed. The increase in the parameter n_0 with the tensile stress suggests the occurrence of the domain refinement and more coherent wall motion. Although n_0 drops slightly with compression, conclusive analysis cannot be done for the compressive stress.

Finally, viewing the results obtained in Fig. 4 and 5, it is obvious that the excess power loss modeled with *Model 1* is better than that obtained from *Model 2*. However, the advantage of *Model 2* is that it only requires the information of H_{hy} (*i.e.* W_{hy}) and its stress dependency in order to obtain fairly good estimation of the stress dependent excess power loss.

VI. Conclusion

Two variants of the excess loss model, both based on the statistical loss theory, were discussed and fitted against measured results. The linear correlation between the model parameters V_0 and the average hysteresis field H_{hy} was validated by the measurements done at wide range of magnetic flux density, frequency and stress combinations. It was concluded from the study and the experimental validation of *Model 1* that the knowledge of only the stress dependent parameter $\big($*i.e.* $n_0(\sigma)\big)$ along with the stress dependent hysteresis loss were sufficient to accurately estimate the stress dependent excess loss. The second variant of the model *Model 2* assuming $n_0 = 0$ (for non-oriented electrical steel) was also studied. In this model as well, only the information of the stress dependent hysteresis loss was sufficient to predict the stress dependent excess loss, albeit with reduced accuracy.

Acknowledgment

The research leading to these results has received funding from the European Research Council under the European Union's Seventh Framework Programme (FP7/2007-2013) / ERC grant agreement n°339380. The authors thank the Finnish Foundation for Technology Promotion (TES), CLEEN Ltd., and the Academy of Finland for their financial support.

References

[1] IEC 60404-2, "Methods of measurement of the magnetic properties of electrical steel strip and sheet by means of an epstein frame," 2008.

[2] IEC 60404-3, "Methods of measurement of the magnetic properties of electrical steel strip and sheet by means of a single sheet tester," 2000.

[3] K. Fujisaki, R. Hirayama, T. Kawachi, S. Satou, C. Kaidou, M. Yabumoto, and T. Kubota, "Motor core iron loss analysis evaluating shrink fitting and stamping by finite-element method," *IEEE Transactions on Magnetics*, vol. 43, pp. 1950–1954, May 2007.

[4] D. Miyagi, K. Miki, M. Nakano, and N. Takahashi, "Influence of compressive stress on magnetic properties of laminated electrical steel sheets," *IEEE Transactions on Magnetics,*, vol. 46, pp. 318–321, Feb 2010.

[5] Y. Kai, Y. Tsuchida, T. Todaka, and M. Enokizono, "Influence of stress on vector magnetic property under alternating magnetic flux conditions," *IEEE Transactions on Magnetics*, vol. 47, pp. 4344–4347, Oct 2011.

[6] Y. Kai, Y. Tsuchida, T. Todaka, and M. Enokizono, "Influence of stress on vector magnetic property under rotating magnetic flux conditions," *IEEE Transactions on Magnetics*, vol. 48, pp. 1421–1424, Apr 2012.

[7] J. B. Goodenough, "A theory of domain creation and coercive force in polycrystalline ferromagnetics," *Phys. Rev.*, vol. 95, pp. 917–932, Aug 1954.

[8] V. Permiakov, L. Dupré, A. Pulnikov, and J. Melkebeek, "Loss separation and parameters for hysteresis modelling under compressive and tensile stresses," *Journal of Magnetism and Magnetic Materials*, vol. 272276, Supplement, no. 0, pp. E553 – E554, 2004. Proceedings of the International Conference on Magnetism (ICM 2003).

[9] G. Bertotti, "General properties of power losses in soft ferromagnetic materials," *IEEE Transactions on Magnetics*, vol. 24, pp. 621–630, Jan 1988.

[10] G. Bertotti, "Physical interpretation of eddy current losses in ferromagnetic materials. i. theoretical considerations," *Journal of Applied Physics*, vol. 57, no. 6, pp. 2110–2117, 1985.

[11] D. Kowal, P. Sergeant, L. Dupré, and L. Vandenbossche, "Comparison of iron loss models for electrical machines with different frequency domain and time domain methods for excess loss prediction," *IEEE Transactions on Magnetics*, vol. 51, pp. 1–10, Jan 2015.

[12] G. Bertotti, "Physical interpretation of eddy current losses in ferromagnetic materials. ii. analysis of experimental results," *Journal of Applied Physics*, vol. 57, no. 6, pp. 2118–2126, 1985.